



OPEN

# Cooperative triple catalysis enables regioirregular formal Mizoroki–Heck reactions

Kun Liu, Dirk Leifert and Armido Studer

**The Mizoroki–Heck reaction between alkenes and aryl halides represents one of the most important methods for C–C bond formation in synthetic chemistry. Governed by their electronic and steric nature, alkenes are generally arylated with high regioselectivity, which conversely hampers diversity, in particular, if the regioirregular isomer is targeted. Usually, electron-poor alkenes selectively afford the corresponding  $\beta$ -coupled products, and achieving the opposite regioselectivity to obtain their  $\alpha$ -arylated congeners is highly challenging. It would be desirable to access the irregular  $\alpha$ -regioisomer by simple variation of the reaction conditions, keeping the standard substrates, thereby significantly enlarging the product space. Herein, we describe an intermolecular  $\alpha$ -arylation of electron-poor alkenes through cooperative nickel, photoredox and sulfinate catalysis. This triple catalysis system operates under mild conditions and features excellent functional group tolerance. The orchestration of radical, transition metal and ionic bond-forming and -cleaving reactions in a single process is highly challenging, but certainly opens valuable doors in terms of reactivity. Moreover, the intermolecular  $\alpha$ -arylation,  $\alpha$ -alkenylation and  $\alpha$ -alkynylation of styrenes could also be achieved through a one-pot process.**

Developing selective and sustainable synthetic methodologies is of great importance in modern organic synthesis<sup>1–3</sup>. Along these lines, transition metal catalysis has played a key role, as recognized by the awarding of the Nobel prize for various reactions<sup>4–7</sup>. For example, the palladium-catalysed Mizoroki–Heck coupling reaction, enabling the arylation of alkenes using aryl (pseudo)halides, represents one of the most versatile and popular tools for the preparation of pharmaceuticals, agrochemicals and advanced materials<sup>8–10</sup>. As the organopalladium insertion step is controlled by the electronic and steric nature of the alkene coupling partner, alkenes bearing electron-donating groups (EDG), such as vinyl ethers and enamides, normally give 1,1-disubstituted alkenes by highly selective  $\alpha$ -coupling (Fig. 1a)<sup>11–13</sup>. Electron-neutral alkenes, such as aliphatic alkenes, often afford a mixture of regioisomers with low selectivity, typically favouring the linear regioisomer<sup>14</sup>. Considering the intrinsic regioselectivity of Mizoroki–Heck couplings, it would be highly desirable to access the irregular regioisomer of the omnipresent Mizoroki–Heck reaction, ideally by simple variation of the reaction conditions, keeping the standard substrates, thereby significantly enlarging the product space. Indeed, by manipulating the transition metal catalyst, ligand and/or aryl pseudohalide substrate, good  $\alpha$ - and  $\beta$ -regioselectivities can be achieved for both electron-rich and aliphatic alkenes<sup>15–23</sup>. However, electron-poor alkenes, such as acrylates and styrenes, which are probably the most widely used starting alkenes in the Mizoroki–Heck coupling reaction, usually furnish the corresponding  $\beta$ -coupling products highly selectively and, due to the dominating electronic factors, achieving the opposite regioselective insertion to obtain the corresponding  $\alpha$ -arylation products is highly challenging<sup>24,25</sup>.

Despite significant achievements in this area, no general solution for the  $\alpha$ -selective coupling of acrylates has been offered to date. To our knowledge, only two examples based on Pd catalysis have been reported to realize regioirregular Mizoroki–Heck reactions. In 2011, Göttker-Schnetmann and co-workers disclosed an interesting  $\alpha$ -phenylation of methyl acrylate using a rather complex organopalladium species as a stoichiometric reagent (Fig. 1b)<sup>26</sup>.

Very recently, Leyva-Pérez and co-workers found that a designed palladium cluster enables the selective intramolecular  $\alpha$ -arylation of electron-deficient alkenes, directly providing valuable unsaturated lactones (Fig. 1c)<sup>27</sup>. However, the use of complex palladium catalysts, high temperatures, a large excess of the alkene coupling partner and/or restriction to the intramolecular variant largely limit the broad application of these elegant processes. Therefore, a general catalytic method for the regioselective intermolecular  $\alpha$ -arylation of acrylates or derivatives thereof with commercially available aryl halides is still highly demanded.

In contrast to the palladium catalysis that dominates regular Mizoroki–Heck reactions, cheap and earth-abundant and non-toxic nickel catalysis has not often been used in such transformations<sup>28,29</sup>. Due to the problematic  $\beta$ -hydride elimination and Ni–H reductive elimination encountered in Ni-catalysed Mizoroki–Heck reactions, harsh conditions and complex ligands are usually required in these reactions<sup>30</sup>. On the other hand, recent developments in Ni-catalysed C–C bond formation have taken advantage of the unique characteristics of nickel as compared with palladium, such as sluggish  $\beta$ -hydride elimination and the tendency to engage in single-electron transfer processes, to enable otherwise inaccessible reactivity<sup>31</sup>. Along this line, dual photoredox and nickel catalysis has shown great potential in the design of co-catalysis strategies for the construction of challenging chemical bonds starting from inexpensive substrates under very mild conditions<sup>32–47</sup>. Inspired by elegant reports on nickel/photoredox dual catalysis<sup>48–64</sup> and our recent work<sup>65</sup>, we envisioned an unprecedented triple catalysis process comprising cooperative nickel, photoredox and sulfinate catalysis to accomplish the challenging intermolecular  $\alpha$ -arylation of electron-deficient alkenes and styrenes using commercially available aryl bromides (Fig. 1d).

Our reaction design to achieve this challenging goal is illustrated in Fig. 1e. An excited photoredox catalyst should first oxidize an arenesulfinate salt by single-electron transfer (SET) to afford an arylsulfonyl radical. Regioselective radical addition of the sulfonyl radical to an electron-deficient alkene **1** will then generate the adduct radical **A**<sup>66–69</sup>. On the other hand, oxidative addition of

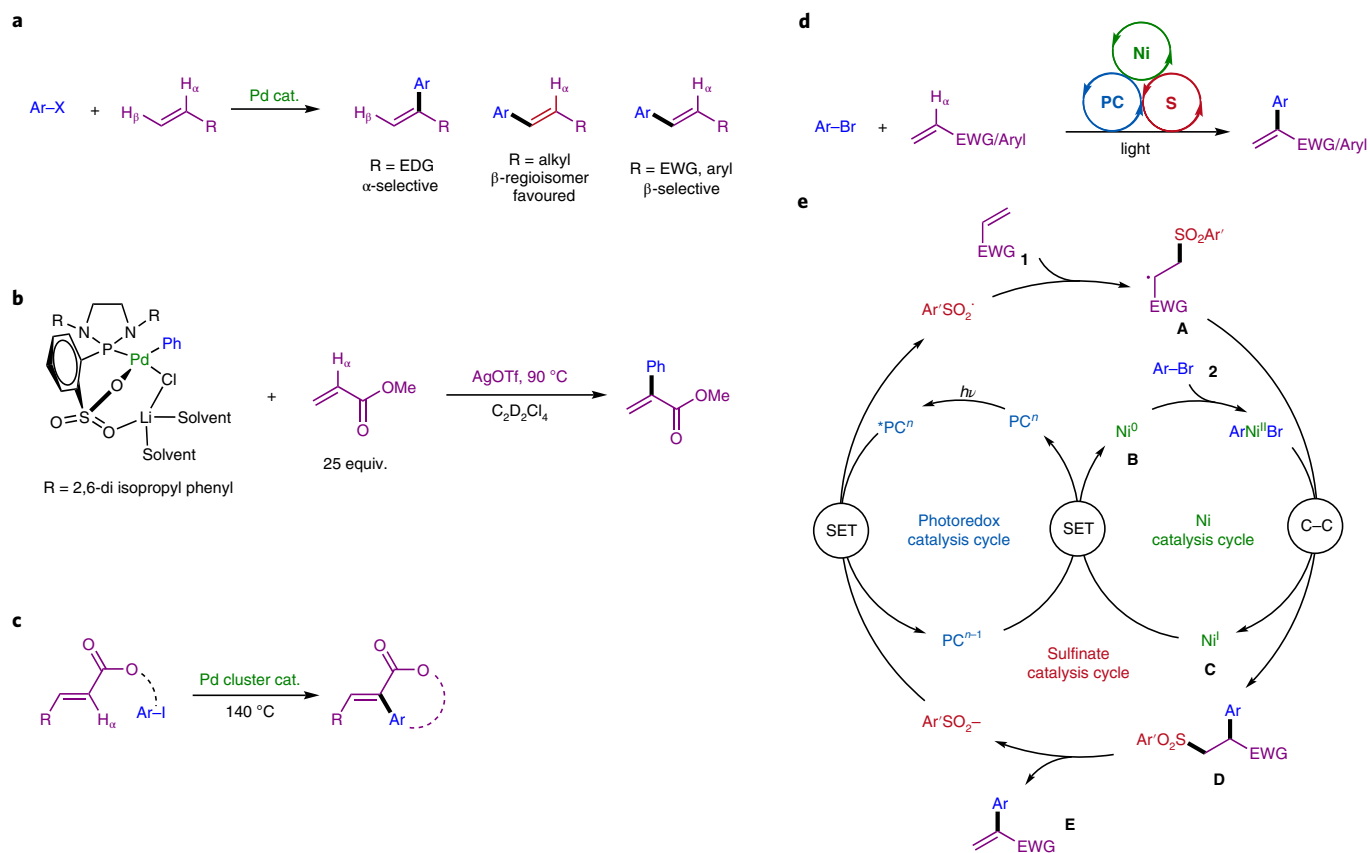


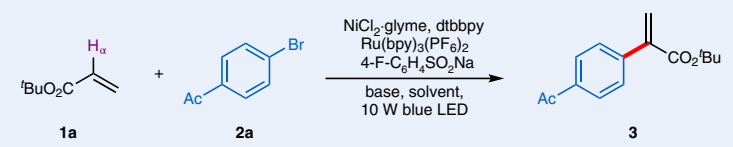
**Fig. 1 | Regioselectivity in the Mizoroki–Heck reaction and strategies for regioirregular coupling of electron-deficient alkenes.** **a**, Intrinsic regioselectivity of the Mizoroki–Heck reaction for different alkenes<sup>10</sup>. **b**, Stoichiometric Pd-mediated regioirregular Mizoroki–Heck reaction of methyl acrylate<sup>26</sup>. **c**, Pd cluster-catalysed intramolecular α-arylation of electron-deficient alkenes to synthesize lactones<sup>27</sup>. **d**, This work: cooperative triple catalysis with nickel, sulfinate and photoredox catalysis enables the intermolecular α-arylation of electron-deficient alkenes and styrenes. **e**, Reaction design and mechanistic proposal with three interwoven catalysis cycles. cat., catalyst; PC, photoredox catalyst; S, sulfinate.

Ni(0) to an aromatic bromide **2** leads to an Ar–Ni–Br complex<sup>70–73</sup>. Trapping of radical **A** by the Ar–Ni–Br species will provide the corresponding Ar–Ni(III)–alkyl intermediate, and subsequent reductive elimination will deliver the intermediate **D** along with a Ni(I) complex<sup>74–77</sup>. Alternatively, the Ni(0) complex might react with radical **A** prior to oxidative addition to the aryl bromide, that is, in reverse order (not shown in Fig. 1e). SET reduction of the Ni(I) species by the initially reduced photoredox catalyst (PC<sup>n-1</sup> complex) will lead to the Ni(0) species and restore the initial PC oxidation state, thereby closing both the PC and Ni catalysis cycles. Finally, base-mediated elimination of the aromatic sulfinate should afford the targeted α-arylated alkene **E**, closing the sulfinate catalysis cycle. Notably, such α-arylated electron-deficient alkenes are prevalent in natural products and also appear as useful intermediates in organic synthesis, rendering our suggested sequence highly valuable with many potential applications<sup>78</sup>.

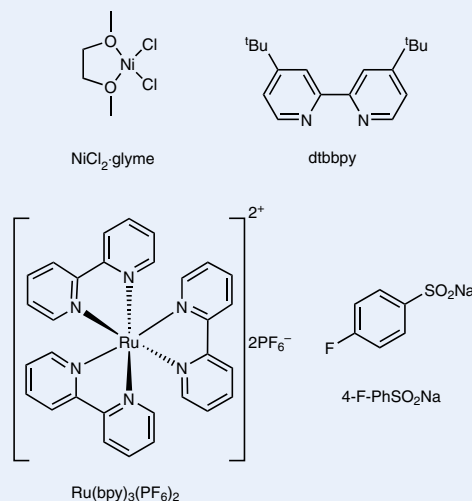
## Results and discussion

**Reaction optimization.** We commenced the investigations with *tert*-butyl acrylate (**1a**) and 1-(4-bromophenyl)ethanone (**2a**) as model substrates. Initially, Ru(bpy)<sub>3</sub>(PF<sub>6</sub>)<sub>2</sub> (bpy denotes 2,2′-bipyridine) was selected as the photoredox catalyst with *para*-fluorobenzene-sulfinate as the co-catalyst, Na<sub>3</sub>PO<sub>4</sub> as the base and dimethylsulfoxide (DMSO) as the solvent. Screening of the metal catalysis with different ligands identified NiCl<sub>2</sub>·glyme and 4,4′-di-*tert*-butyl-2,2′-bipyridine (dtbbpy) as the most suitable combination in this series, and the desired α-arylation product **3** was obtained in a promising

26% yield with exclusive α-selectivity (Table 1, entry 1). No or only a trace amount of the product was identified if stronger bases such as Cs<sub>2</sub>CO<sub>3</sub> or 1,8-diazabicyclo[5.4.0]undec-7-ene (DBU) were used in place of Na<sub>3</sub>PO<sub>4</sub> (Table 1, entries 2 and 3). Furthermore, increasing the amount of Na<sub>3</sub>PO<sub>4</sub> led to higher substrate conversion, but a reduced yield; trace amounts of unknown products were identified (Table 1, entry 4). To our delight, 0.85 equiv. bis(pinacolato)diboron (B<sub>2</sub>pin<sub>2</sub>) as an additive improved the reaction efficiency and **3** was obtained in 58% yield (Table 1, entry 5). However, replacing B<sub>2</sub>pin<sub>2</sub> with other boron compounds, such as benzylboronic acid pinacol ester (BnBpin), B<sub>2</sub>(OH)<sub>4</sub> or bis(catecholato)diboron (B<sub>2</sub>Cat<sub>2</sub>), provided worse results (Table 1, entry 6). As a side reaction, cross-coupling between 1-(4-bromophenyl)ethanone and *para*-fluorobenzene-sulfinate occurred in these transformations, which led to the consumption of the sulfinate catalyst. We also tested various solvent mixtures, with α-arylation in DMSO–tetrahydrofuran (THF) providing nearly the same result (Table 1, entry 7). A slight improvement in yield was noted upon running the arylation in DMSO–MeCN (Table 1, entry 8). Pleasingly, we found that the cascade reaction occurred most efficiently in DMSO–*N,N*-dimethylformamide (DMF; 3:2), with the α-arylation product **3** isolated in 74% yield (Table 1, entry 9). Of note, the side reaction was almost fully suppressed in this solvent system. Finally, control experiments revealed that the photoredox catalyst, nickel catalyst, ligand, sulfinate, irradiation and base were all indispensable to obtain the desired product (Table 1, entry 10). Importantly, in all successful reactions, **3** was formed with exclusive α-selectivity.

**Table 1 | Optimization of the reaction conditions for the  $\alpha$ -arylation of alkenes**


Entry	Base	Solvent	Yield of <b>3</b> (%)
1	Na <sub>3</sub> PO <sub>4</sub> (0.6 equiv.)	DMSO	26
2	Cs <sub>2</sub> CO <sub>3</sub> (0.6 equiv.)	DMSO	Trace
3	DBU (0.6 equiv.)	DMSO	ND
4	Na <sub>3</sub> PO <sub>4</sub> (1.1 equiv.)	DMSO	9
5 <sup>a</sup>	Na <sub>3</sub> PO <sub>4</sub> (1.1 equiv.)	DMSO	58
6 <sup>b</sup>	Na <sub>3</sub> PO <sub>4</sub> (1.1 equiv.)	DMSO	15–33
7 <sup>a</sup>	Na <sub>3</sub> PO <sub>4</sub> (1.1 equiv.)	DMSO–THF (0.6:0.4)	55
8 <sup>a</sup>	Na <sub>3</sub> PO <sub>4</sub> (1.1 equiv.)	DMSO–MeCN (0.6:0.4)	62
9 <sup>a</sup>	Na <sub>3</sub> PO <sub>4</sub> (1.1 equiv.)	DMSO–DMF (0.6:0.4)	74
10 <sup>c</sup>	Na <sub>3</sub> PO <sub>4</sub> (1.1 equiv.)	DMSO–DMF (0.6:0.4)	ND



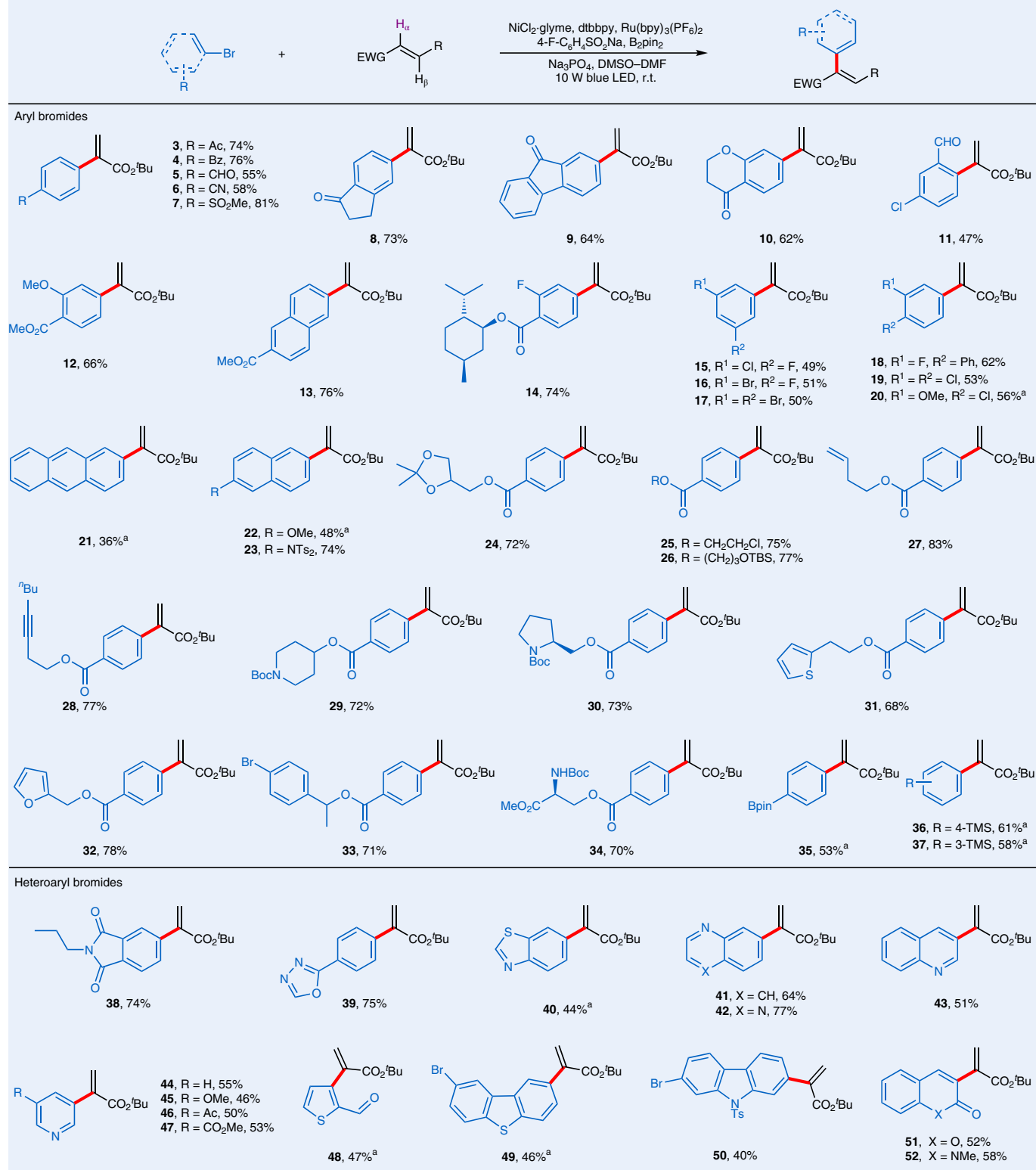
Reaction conditions: **1a** (0.3 mmol), **2a** (0.15 mmol), NiCl<sub>2</sub>.glyme (10 mol%), dtbbpy (15 mol%), Ru(bpy)<sub>3</sub>(PF<sub>6</sub>)<sub>2</sub> (1 mol%), 4-F-C<sub>6</sub>H<sub>4</sub>SO<sub>2</sub>Na (30 mol%), base (0.6 equiv.) and solvent (1.5 ml) under irradiation with a 10 W blue light-emitting diode (LED) for 24 h. <sup>a</sup>B<sub>2</sub>pin<sub>2</sub> (0.85 equiv.) was added as additive. <sup>b</sup>BnBpin, B<sub>2</sub>(OH)<sub>4</sub> or B<sub>2</sub>Cat<sub>2</sub> was added as additive in place of B<sub>2</sub>pin<sub>2</sub>. <sup>c</sup>If the photoredox catalyst, nickel catalyst, ligand, sulfinate, irradiation or base was omitted, the reaction did not proceed. ND, not detected.

**Substrate scope.** To evaluate the generality of this protocol, we systematically investigated the substrate scope. First, the effect of substituents on the benzene ring in various aryl bromides was studied, keeping *tert*-butyl acrylate (**1a**) as the coupling partner (Table 2). Aryl bromides bearing electron-withdrawing groups (EWGs), including acyl, formyl, methoxycarbonyl, cyano and methylsulfonyl, reacted smoothly and the corresponding  $\alpha$ -arylated alkenes **3–13** were obtained in moderate-to-very-good yields (47–81%). As expected, chloro- and fluorobenzenes also reacted with complete chemoselectivity (**14–19**). Considering polybrominated benzenes, the mono- $\alpha$ -arylation products **16** and **17** were selectively formed with the additional C–Br bonds remaining untouched. Moreover, electron-rich aryl bromides also reacted to give alkene adducts (**20–23**). Additional functional groups, such as ketal, primary alkyl chloride, *tert*-butyldimethylsilyl (TBS)-protected hydroxy, terminal alkene, internal alkyne, amide, amino acid ester, furan, thiophene and benzylic ester, were all well tolerated (**24–34**). Remarkably, this transformation is also compatible with other conventional cross-coupling-enabling functionalities. For example, high chemoselectivity was achieved in the  $\alpha$ -arylation reaction with aryl bromides carrying a boronic ester moiety. Thus, alkene **35** with the boronic acid pinacol ester (Bpin) functionality untouched could be prepared (53%). Acrylates **36** and **37** with an intact Me<sub>3</sub>SiAr entity could also be prepared (58–61%). Moreover, this method also offers direct access to a wide range of  $\alpha$ -heteroaryl-substituted acrylates, with phthalimide, oxadiazole, benzothiazole, quinoline, quinoxaline, pyridine, thiophene, dibenzothiophene as well as carbazole moieties being installed by this strategy (**38–50**, 40–77%). Furthermore, brominated coumarin and 2-quinolone could be successfully used as aryl donors for the preparation of the corresponding 1,3-diene derivatives **51** and **52**.

The generality of the  $\alpha$ -arylation reaction was further evaluated by exploring the scope with respect to the alkene acceptor (Table 3). The ester substituent of the acrylate could be readily varied, as

documented by the successful direct synthesis of the  $\alpha$ -arylated acrylates **53–59** (66–76%). However, crotonates reacted with lower efficiency, likely due to steric effects (**60**). The  $\alpha$ -arylation reaction also proceeded with acrylonitrile, vinylphosphonate and an acrylamide as acceptors, albeit in lower yields (**61–63**). Unfortunately, other electron-deficient alkenes, such as phenyl vinyl sulfone, methyl vinyl ketone, 2-cyclopenten-1-one and 2(5*H*)-furanone, failed to afford the corresponding  $\alpha$ -arylation products (Supporting Information). In the reaction with the vinyl ketone, we observed only the radical addition of the sulfonyl radical to the vinyl ketone (Giese reaction product). With regard to unactivated alkenes such as 1-hexene, neither radical addition nor difunctionalization products were detected. Next, we probed a range of more complex aryl bromides and acrylates to demonstrate the suitability of the method for late-stage functionalization. Substrates derived from *D*-allofurano-*n*ose, vanillin, tocopherol and cholesterol all reacted smoothly to provide the desired products in good yields (**64–67**).

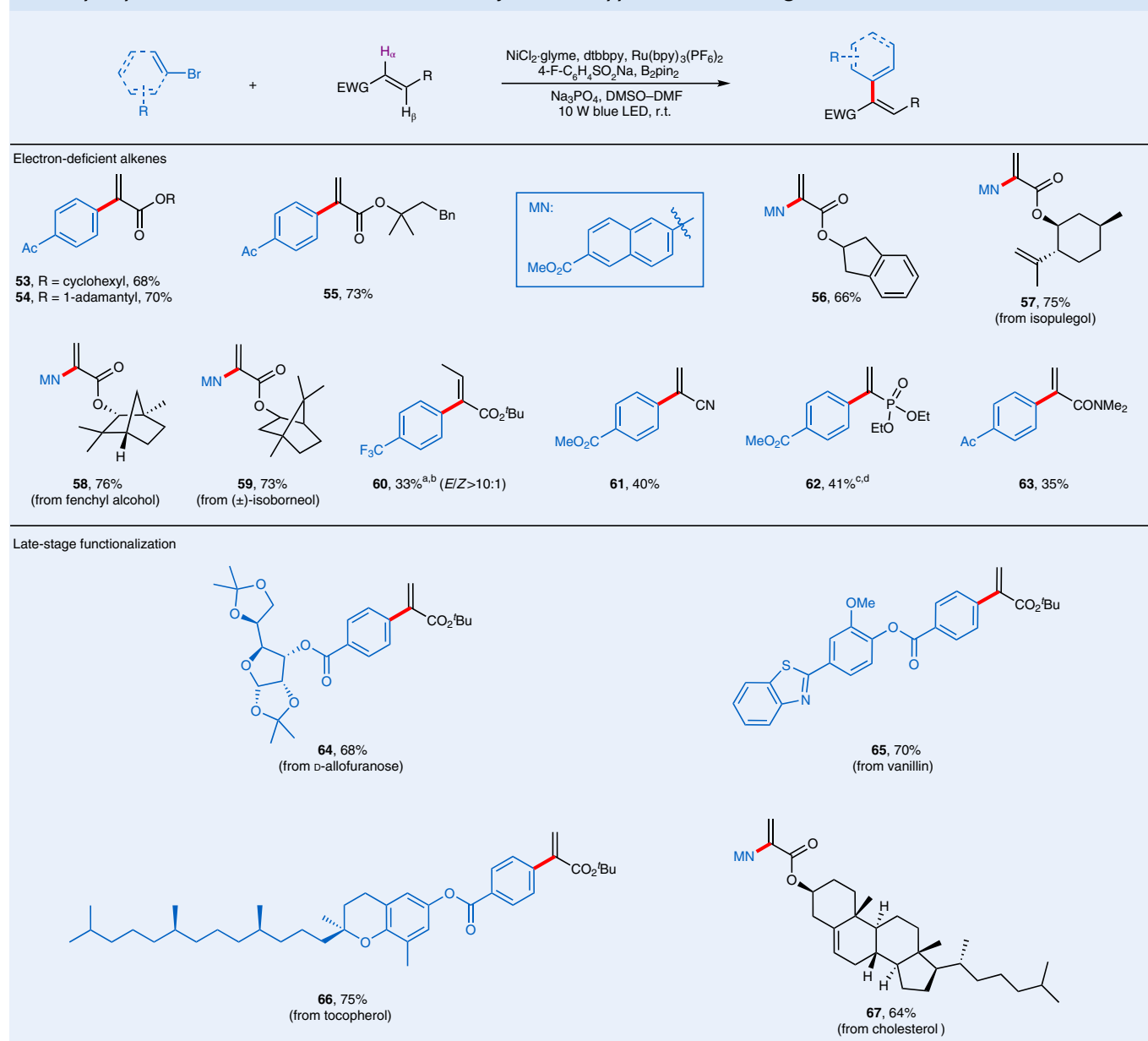
We continued our studies by exploring the intermolecular  $\alpha$ -arylation of styrenes to access 1,1-diarylalkenes (Table 4). These investigations were conducted with 4-bromobenzophenone as the coupling partner. We found that the reaction with *para*-trifluoromethylstyrene did not proceed under the conditions optimized for acrylate arylation. The problematic step was the base-mediated elimination of sulfinate, due to the lower acidity of the  $\alpha$ -proton in the intermediate aryl sulfone. Careful experimentation identified DBU as the ideal base for this elimination. However, DBU was not compatible with the first two steps of the cascade reaction (1,2-difunctionalization). This revised protocol was employed for the arylation of all the systems in this study. Therefore, a one-pot protocol was developed with DBU treatment after the initial cooperative photoredox/Ni-catalysed 1,2-difunctionalization, and the targeted **68** was isolated in 66% yield. The *p*-MeO<sub>2</sub>C-substituted congener reacted with similar efficiency (**69**). Styrene acceptors bearing halogen atoms at different positions of the arene moiety

**Table 2 | Scope for (hetero)aryl bromides in the  $\alpha$ -arylation reaction**

Reactions were conducted on a scale of 0.15 mmol. The yields correspond to the isolated material after purification. Reaction conditions: aryl bromide (0.15 mmol), alkene (0.3 mmol), NiCl<sub>2</sub>.glyme (10 mol%), dtbbpy (15 mol%), Ru(bpy)<sub>3</sub>(PF<sub>6</sub>)<sub>2</sub> (1 mol%), 4-F-C<sub>6</sub>H<sub>4</sub>SO<sub>2</sub>Na (30 mol%), B<sub>2</sub>pin<sub>2</sub> (0.85 equiv.), Na<sub>3</sub>PO<sub>4</sub> (1.1 equiv.) and DMSO-DMF (0.9:0.6 ml) under irradiation with a 10 W blue LED for 24 h. See the Supplementary Information for details. <sup>a</sup>The reaction was performed for 30 h. r.t., room temperature; Bz, benzoyl; Boc, *tert*-butoxycarbonyl; TMS, trimethylsilyl.

could also be transformed to afford the corresponding products **70–74** in yields of 51–74%. For more electron-rich styrenes containing *p*-methoxy and benzofuran entities, the  $\alpha$ -arylation proceeded

with lower yields (**75** and **76**). Moreover, a benzylic ester as side chain was also tolerated (**77**), and alkenes derived from important drugs such as fenofibrate and oestrone could be selectively arylated

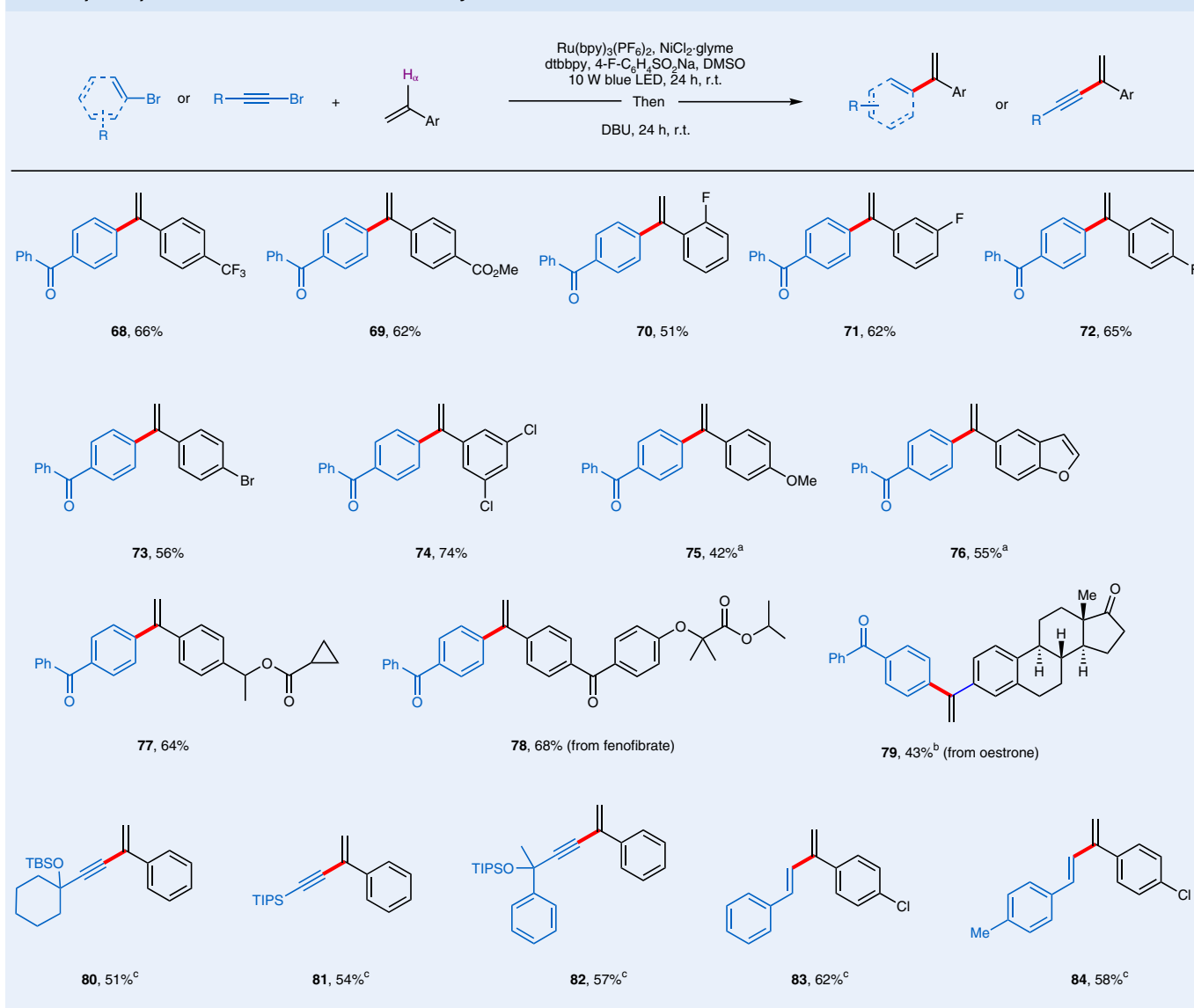
**Table 3 | Scope for electron-deficient alkenes in the  $\alpha$ -arylation and application to late-stage functionalization**

Reactions were conducted on a 0.15 mmol scale. The yields correspond to the isolated material after purification. Reaction conditions: aryl bromide (0.15 mmol), alkene (0.3 mmol), NiCl<sub>2</sub>.glyme (10 mol%), dtbbpy (15 mol%), Ru(bpy)<sub>3</sub>(PF<sub>6</sub>)<sub>2</sub> (1 mol%), 4-F-C<sub>6</sub>H<sub>4</sub>SO<sub>2</sub>Na (30 mol%), B<sub>2</sub>pin<sub>2</sub> (0.85 equiv.), Na<sub>3</sub>PO<sub>4</sub> (1.1 equiv.) and DMSO-DMF (0.9:0.6 ml) under irradiation with a 10 W blue LED for 24 h. See the Supplementary Information for details. <sup>a</sup>The reaction was performed for 30 h. <sup>b</sup>4-CF<sub>3</sub>-C<sub>6</sub>H<sub>4</sub>SO<sub>2</sub>Na was used instead of 4-F-C<sub>6</sub>H<sub>4</sub>SO<sub>2</sub>Na. <sup>c</sup>PhSO<sub>2</sub>Na was used instead of 4-F-C<sub>6</sub>H<sub>4</sub>SO<sub>2</sub>Na. <sup>d</sup>For this reaction, 1.0 equiv. B<sub>2</sub>pin<sub>2</sub> was used.

at the  $\alpha$ -position (**78** and **79**). It is important to note that by applying this second strategy, the cascade reaction can be stopped at the 1,2-difunctionalization stage by just leaving out the final DBU treatment to obtain arylsulfones of type **D** (see Fig. 1e and the mechanistic studies below). Along with aryl bromides, we were delighted to discover that bromoalkynes as well as (*E*)-bromoalkenes are also eligible electrophiles for this transformation, with these substrates furnishing a variety of interesting 1,3-enynes and 1,3-dienes (**80–84**).

The practicality and synthetic potential of the  $\alpha$ -arylation of acrylates were then explored (Fig. 2). The robustness was documented by repeating four reactions on a larger scale, with comparable yields being obtained in all cases (**18** (51%), **3** (73%), **13** (72%) and **20** (51%)). The synthetic value of this methodology was further highlighted by synthesizing some medically interesting compounds through chemical modification of the  $\alpha$ -arylated acrylates.

For example, the *tert*-butyl ester moiety in **18** can be cleaved to provide the corresponding acrylic acid **85** in near quantitative yield. The known asymmetric hydrogenation of this acid would directly lead to flurbiprofen, which is an important anti-pain and anti-inflammatory agent (Fig. 2a)<sup>79</sup>. Nucleophilic addition of pyrrole to the double bond of **18** furnished the ester **86**, which is a key intermediate in the preparation of an ipalbidine variant<sup>80</sup>. Base-promoted [4+2] annulation of **18** with malononitrile delivered the polysubstituted pyridinone **87** in 54% yield, which can be used for the preparation of an epidermal growth factor inhibitor derivative<sup>81</sup>. Moreover, the polysubstituted 4,5-dihydroisoxazole **88** was obtained in 75% yield by [3+2] annulation of **3** with 1-nitropropane (Fig. 2b)<sup>82</sup>. The tilidine variant **89**, a derivative of a synthetic opioid painkiller, was easily accessed by [4+2] annulation of an enamine with **3** (ref. <sup>83</sup>). Iodine-catalysed cyclopropanation of **13** with a diazo ester afforded

**Table 4 | One-pot  $\alpha$ -functionalization of various styrenes**

Reactions were conducted on a 0.1 mmol scale. The yields refer to the isolated material after purification. Reaction conditions: (4-bromophenyl)(phenyl)methane (0.1 mmol), styrene derivative (0.2 mmol), 4-F-C<sub>6</sub>H<sub>4</sub>SO<sub>2</sub>Na (0.1 mmol), NiCl<sub>2</sub>·glyme (10 mol%), dtbbpy (15 mol%), Ru(bpy)<sub>3</sub>(PF<sub>6</sub>)<sub>2</sub> (1 mol%) and DMSO (1 ml) under irradiation with a 10 W blue LED for 24 h at r.t.; then, DBU (0.3 mmol, 3 equiv.) under argon and stirring for 24 h at r.t. See the Supplementary Information for details. <sup>a</sup>The second step was performed for 32 h. <sup>b</sup>7-Methyl-1,5,7-triazabicyclo[4.4.0]dec-5-ene (0.3 mmol, 3 equiv.) was used instead of DBU. <sup>c</sup>Reaction conditions: bromoalkyne or bromoalkene (0.1 mmol), styrene derivative (0.2 mmol), 4-F-C<sub>6</sub>H<sub>4</sub>SO<sub>2</sub>Na (0.1 mmol), NiBr<sub>2</sub>·3H<sub>2</sub>O (10 mol%), bathocuproin (15 mol%), Ir(dtbbpy)(ppy)<sub>2</sub>PF<sub>6</sub> (ppy denotes 2-phenylpyridine) (1 mol%) and DMF (1 ml) under irradiation with a 10 W blue LED for 24 h; then, DBU (0.3 mmol, 3 equiv.) under argon and stirring at 40 °C for 24 h. TIPS, triisopropylsilyl.

the corresponding cyclopropane **90** in a very high yield (Fig. 2c)<sup>84</sup>, and intermolecular hydroamination with benzylamine gave the  $\beta$ -amino acid ester **91** in 83% yield. In addition, an intermediate (**92**) in the preparation of an (*S*)-equol derivative was successfully prepared by Pd-catalysed arylation of **20** with an arenediazonium salt. Subsequent hydrolysis, asymmetric hydrogenation and deprotection, as described previously, would then lead to the (*S*)-equol derivative (Fig. 2d)<sup>85</sup>.

**Mechanistic studies.** To support the mechanistic proposal depicted in Fig. 1e, additional experiments were conducted. First, the addition of 2 equiv. (2,2,6,6-tetramethylpiperidin-1-yl)oxyl (TEMPO) fully suppressed the model reaction (Fig. 3a). The radical nature of this transformation was further supported by the radical probe experiment performed with alkene **93** as the acceptor to furnish the ring-opened product **94** in 87% yield (Fig. 3b). Stern–Volmer

fluorescence quenching experiments revealed that only 4-F-C<sub>6</sub>H<sub>4</sub>SO<sub>2</sub>Na quenched the excited state of Ru\*(II), in accordance with our proposed mechanism (Supplementary Section 7.5). In addition, we found that stoichiometric reaction of the presynthesized Ar–Ni<sup>II</sup>–Br complex<sup>86</sup> (Supplementary Information 7.3) with **1a** afforded the desired product **3** in 41% yield. When a catalytic amount (10 mol%) of the nickel complex was used, the product **3** was formed in 35% yield. These results indicate that this Ni(II) complex might be a competent intermediate in the transformation (Fig. 3c,d). The absence of a hydrosulfonylation product in the reaction of *tert*-butyl acrylate with 4-F-C<sub>6</sub>H<sub>4</sub>SO<sub>2</sub>Na showed that ionic conjugate addition did not occur (Fig. 3e). As described above, in the absence of B<sub>2</sub>pin<sub>2</sub>, the desired product **3** was also formed in the model reaction, albeit in a low yield (26%, Table 1, entry 1). This result shows that the cascade reaction can also proceed without the formation of any potential boron-based intermediate. To further

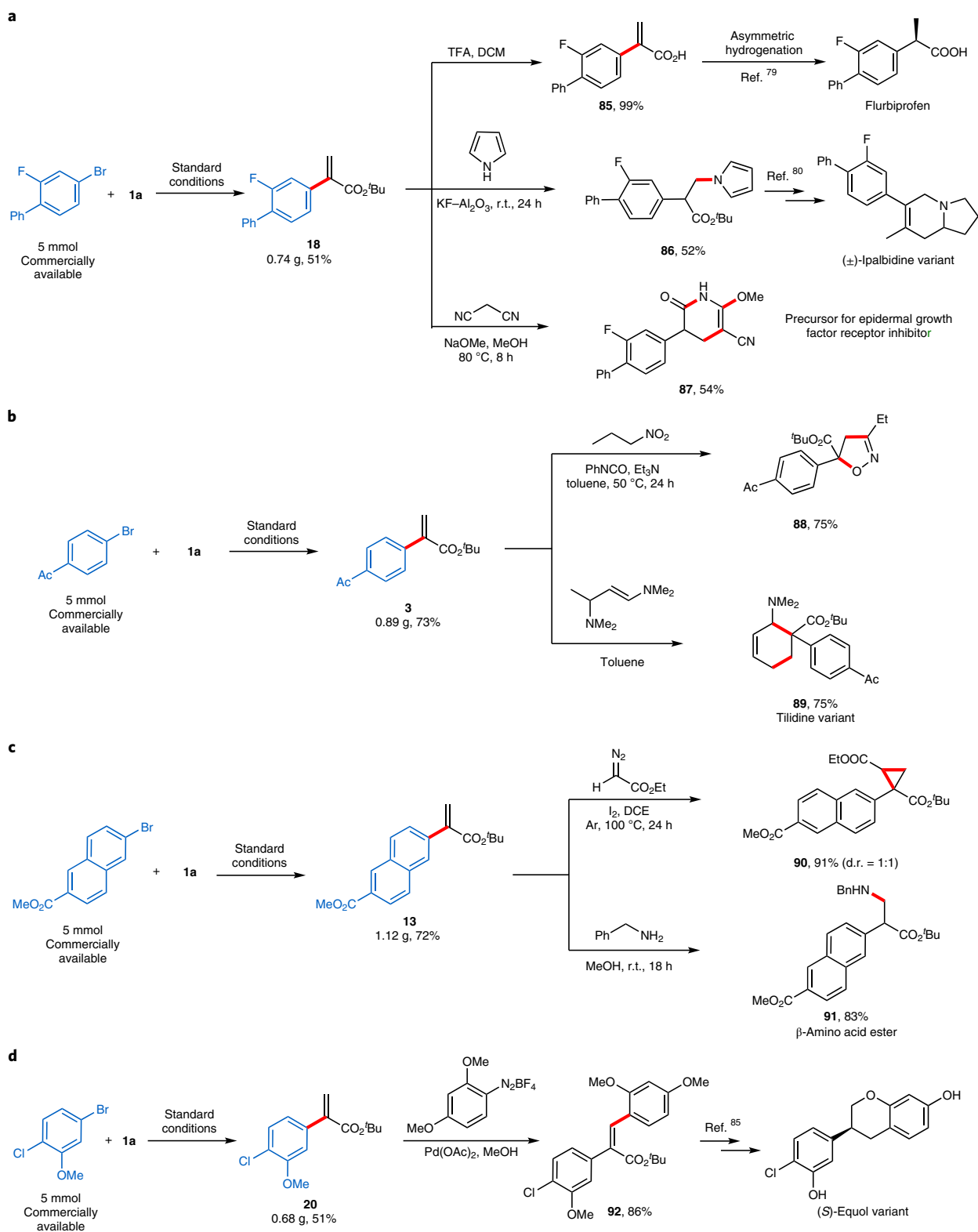


**Fig. 2 | Large-scale synthesis and applications of the  $\alpha$ -arylation reaction.** **a**, Acrylate arylation for the preparation of key intermediates to access the biologically active compounds flurbiprofen, an ipalbidine derivative and a lactam. **b**, Arylated acrylates as substrates for cycloaddition reactions. **c**, Cyclopropanation and  $\beta$ -amination of acrylate **13**. **d**, Formal synthesis of an (*S*)-equol derivative. TFA, trifluoroacetic acid; DCM, dichloromethane; DCE, 1,2-dichloroethane.

explore this issue, an equimolar mixture of the aryl bromide **2a** and 4-NC-C<sub>6</sub>H<sub>4</sub>Bpin was allowed to react under the standard conditions with **1a** in the absence of B<sub>2</sub>pin<sub>2</sub>, giving the product **3** in 12% yield.

Thus, 4-NC-C<sub>6</sub>H<sub>4</sub>Bpin did not participate, which indicates that the aryl bromide and B<sub>2</sub>pin<sub>2</sub> do not react to provide the corresponding arylboronic acid pinacol ester (Fig. 3f).

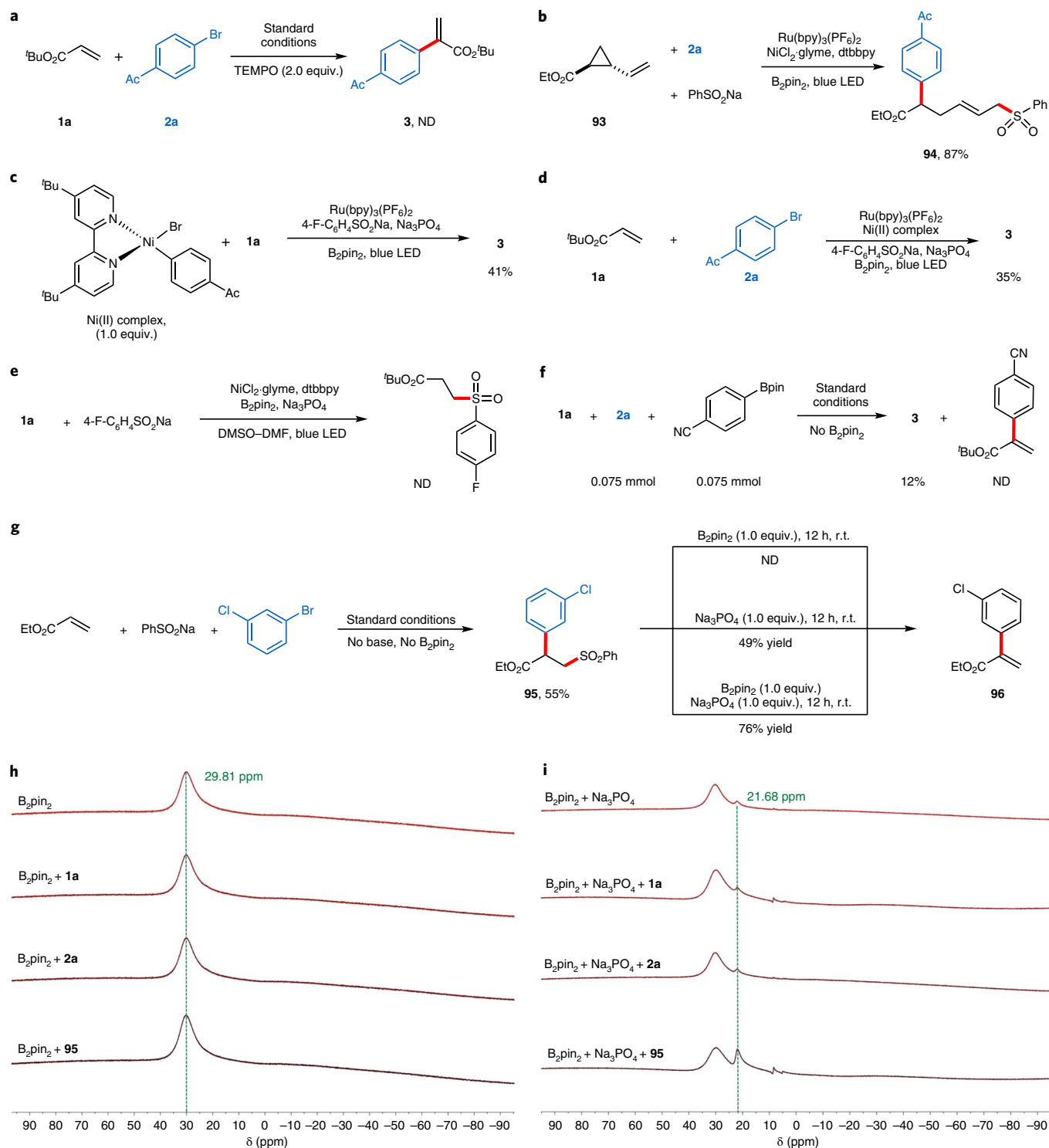


**Fig. 3 | Mechanistic studies.** **a**, The reaction is fully suppressed in the presence of TEMPO. **b**, Radical probe experiment using alkene **93** as the substrate. The radical nature of this reaction is supported by obtaining the ring-opened product **94** in 87% yield. **c**,  $\alpha$ -Arylation using a stoichiometric amount of a preformed Ar-Ni<sup>II</sup>-Br complex. **d**,  $\alpha$ -Arylation using a preformed Ar-Ni<sup>II</sup>-Br complex as catalyst. **e**, Attempted ionic addition of the 4-F-PhSO<sub>2</sub>Na to acceptor **1a**. **f**, Competition experiment performed with an aryl bromide and an arylboronic ester as potential aryl donors. **g**, Three-component coupling and subsequent sulfinate elimination shows that the combination of B<sub>2</sub>pin<sub>2</sub> and Na<sub>3</sub>PO<sub>4</sub> enhances the sulfinate elimination efficiency. **h**, <sup>13</sup>C NMR spectroscopy was used to evaluate the interactions between B<sub>2</sub>pin<sub>2</sub> and individual reactants (**h**) and between B<sub>2</sub>pin<sub>2</sub>, Na<sub>3</sub>PO<sub>4</sub> and individual reactants (**i**).

In addition, we also conducted the reaction between ethyl acrylate and an aryl bromide in the presence of 1 equiv. PhSO<sub>2</sub>Na in the absence of base, which afforded the three-component coupling product **95** in 55% yield (Fig. 3g). To explore the sulfinate

elimination step, intermediate **95** was then treated with B<sub>2</sub>pin<sub>2</sub> (1 equiv.), but the desired product **96** was not detected, whereas a 49% yield of **96** could be obtained on addition of Na<sub>3</sub>PO<sub>4</sub> (1 equiv.). Interestingly, the combined action of B<sub>2</sub>pin<sub>2</sub> and Na<sub>3</sub>PO<sub>4</sub> (1 equiv.



each) enhanced the sulfinate elimination efficiency and **96** was formed in 76% yield within 12 h. Further addressing the effect of  $B_2pin_2$ , we conducted  $^{11}B$  NMR studies in  $[^2H_6]DMSO$  to evaluate any potential interaction between  $B_2pin_2$  and the substrates or products. No change in the  $^{11}B$  NMR shift (29.81 ppm) was observed upon mixing  $B_2pin_2$  with the acrylate **1a**, aryl bromide **2a** or the three-component coupling product **95**, showing that neither the ester moiety nor the bromide forms a Lewis acid–base interaction with  $B_2pin_2$  (Fig. 3h). In contrast, after the addition of 1 equiv.  $Na_3PO_4$  to  $B_2pin_2$ , a small new peak appeared upfield (21.68 ppm), implying the formation of a boronate complex with the phosphate in which  $B_2pin_2$  acts as a Lewis acid. Subsequent addition of **1a** or **2a** to the mixture of  $B_2pin_2$  and  $Na_3PO_4$  did not alter the intensity of the upfield small peak (Fig. 3i). However, the peak at 21.68 ppm from the  $B_2pin_2$ – $Na_3PO_4$  mixture significantly increased in intensity after the addition of intermediate **95**. This indicates that the  $Na_3PO_4$ – $B_2pin_2$  complex is present at higher concentration in the presence of **95**. It is likely that the boron-complexed phosphate shows higher Na Lewis acidity, which might explain why  $B_2pin_2$  facilitates the elimination of the arenesulfinate. Thus, the likely effect of  $B_2pin_2$  on the overall cascade reaction is the acceleration of the ionic sulfinate elimination<sup>87–91</sup>.

## Conclusions

In summary, we have developed a robust method for the intermolecular regioirregular formal Mizoroki–Heck reaction of electron-deficient alkenes and styrenes with readily available aryl bromides. The cascade reaction proceeds by triple catalysis involving nickel catalysis, photoredox catalysis and sulfinate catalysis, with all three catalysis cycles interwoven. A variety of value-added  $\alpha$ -arylated alkenes, 1,3-enynes and 1,3-dienes have been successfully constructed in good yield and with excellent regioselectivity. Mechanistic studies show that these transformations proceed through a radical addition/metal–radical coupling/ionic elimination cascade. We believe that this method offers a solution to a long-standing synthetic challenge, namely the intermolecular  $\alpha$ -arylation of electron-poor alkenes, and should therefore find many applications. Future advances in selective functionalization based on this triple catalysis strategy are foreseen.

## Methods

### General procedure for the $\alpha$ -arylation of electron-deficient alkenes.

$Ru(bpy)_3(PF_6)_2$  (1.3 mg, 1.5  $\mu$ mol, 1.0 mol%),  $NiCl_2 \cdot glyme$  (3.3 mg, 0.015 mmol, 10 mol%), dtbbpy (6.0 mg, 0.023 mmol, 15 mol%), sodium 4-fluorobenzenesulfinate (8.2 mg, 0.045 mmol, 30 mol%),  $B_2pin_2$  (32.5 mg, 0.128 mmol, 0.85 equiv.), aryl bromide (0.15 mmol, 1.0 equiv.) and  $Na_3PO_4$  (27.1 mg, 0.165 mmol, 1.1 equiv.) were added to an oven-dried 10-ml Schlenk tube. The reaction tube was then evacuated and backfilled with argon three times. Next, DMSO (0.9 ml) and DMF (0.6 ml) were added, followed by an alkene (0.30 mmol, 2.0 equiv.). The resulting mixture was stirred for 3 min before irradiating with a 10 W blue LED at room temperature for 24 h. The reaction mixture was diluted with DCM (6 ml) and transferred into a separatory funnel charged with brine (30 ml). The phases were then separated and the aqueous phase was extracted with DCM (2  $\times$  10 ml). The combined organic phases were concentrated and then purified by silica gel chromatography (PE–Et<sub>2</sub>O) to afford the desired product.

**General procedure for the direct one-pot  $\alpha$ -arylation of styrenes.**  $Ru(bpy)_3(PF_6)_2$  (0.9 mg, 1  $\mu$ mol, 1 mol%),  $NiCl_2 \cdot glyme$  (2.2 mg, 0.010 mmol, 10 mol%), dtbbpy (4.0 mg, 0.015 mmol, 15 mol%), sodium 4-fluorobenzenesulfinate (18.2 mg, 0.100 mmol, 1.0 equiv.) and aryl bromide (0.10 mmol, 1.0 equiv.) were added to an oven-dried 10-ml Schlenk tube. The reaction tube was then evacuated and backfilled with argon three times. Next, DMSO (1 ml) was added, followed by the styrene derivative (0.20 mmol, 2.0 equiv.). The resulting mixture was stirred for 3 min before irradiating with a 10 W blue LED at room temperature for 24 h. Under the protection of argon, DBU (0.30 mmol, 3.0 equiv.) was added to the above mixture, which was then stirred at room temperature for another 24 h. Next, the mixture was diluted with DCM (6 ml) and transferred into a separatory funnel charged with brine (30 ml). The phases were then separated and the aqueous phase extracted with DCM (2  $\times$  10 ml). The combined organic phases were concentrated and then purified by silica gel chromatography (PE–Et<sub>2</sub>O) to afford the desired product.

## Data availability

The authors declare that the data supporting the findings of this study are available within the paper and its Supplementary Information.

Received: 22 March 2022; Accepted: 20 May 2022;

Published online: 13 July 2022

## References

- Blakemore, D. C. et al. Organic synthesis provides opportunities to transform drug discovery. *Nat. Chem.* **10**, 383–394 (2018).
- Wender, P. A. & Miller, B. L. Synthesis at the molecular frontier. *Nature* **460**, 197–201 (2009).
- Young, I. S. & Baran, P. S. Protecting-group-free synthesis as an opportunity for invention. *Nat. Chem.* **1**, 193–205 (2009).
- Giri, R., Shi, B.-F., Engle, K. M., Maugel, N. & Yu, J.-Q. Transition metal-catalyzed C–H activation reactions: diastereoselectivity and enantioselectivity. *Chem. Soc. Rev.* **38**, 3242–3272 (2009).
- Johansson Seechurn, C. C. C., Kitching, M. O., Colacot, T. J. & Snieckus, V. Palladium-catalyzed cross-coupling: a historical contextual perspective to the 2010 Nobel Prize. *Angew. Chem. Int. Ed.* **51**, 5062–5085 (2012).
- Miyaura, N. & Suzuki, A. Palladium-catalyzed cross-coupling reactions of organoboron compounds. *Chem. Rev.* **95**, 2457–2483 (1995).
- Trost, B. M. & Crawley, M. L. Asymmetric transition-metal-catalyzed allylic alkylations: applications in total synthesis. *Chem. Rev.* **103**, 2921–2944 (2003).
- Dounay, A. B. & Overman, L. E. The asymmetric intramolecular Heck reaction in natural product total synthesis. *Chem. Rev.* **103**, 2945–2964 (2003).
- Mc Cartney, D. & Guiry, P. J. The asymmetric Heck and related reactions. *Chem. Soc. Rev.* **40**, 5122–5150 (2011).
- Oestreich, M. *The Mizoroki–Heck Reaction* (Wiley, 2009).
- Carrow, B. P. & Hartwig, J. F. Ligandless, anionic, arylpalladium halide intermediates in the Heck reaction. *J. Am. Chem. Soc.* **132**, 79–81 (2010).
- Herrmann, W. A. et al. Palladacycles: efficient new catalysts for the Heck vinylation of aryl halides. *Chem. Eur. J.* **3**, 1357–1364 (1997).
- Ruan, J. & Xiao, J. From  $\alpha$ -arylation of olefins to acylation with aldehydes: a journey in regiocontrol of the Heck reaction. *Acc. Chem. Res.* **44**, 614–626 (2011).
- Dieck, H. A. & Heck, R. F. Organophosphinepalladium complexes as catalysts for vinylic hydrogen substitution reactions. *J. Am. Chem. Soc.* **96**, 1133–1136 (1974).
- Datta, G. K., von Schenck, H., Hallberg, A. & Larhed, M. Selective terminal Heck arylation of vinyl ethers with aryl chlorides: a combined experimental–computational approach including synthesis of betaxolol. *J. Org. Chem.* **71**, 3896–3903 (2006).
- Domzalska-Pieczkolan, A., Funes-Ardoiz, I., Furman, B. & Bolm, C. Selective approaches to  $\alpha$ - and  $\beta$ -arylated vinyl ethers. *Angew. Chem. Int. Ed.* **61**, e202109801 (2022).
- Lv, H. et al. Nickel-catalyzed intermolecular oxidative Heck arylation driven by transfer hydrogenation. *Nat. Commun.* **10**, 5025 (2019).
- Qin, L., Ren, X., Lu, Y., Li, Y. & Zhou, J. Intermolecular Mizoroki–Heck reaction of aliphatic olefins with high selectivity for substitution at the internal position. *Angew. Chem. Int. Ed.* **51**, 5915–5919 (2012).
- Standley, E. A. & Jamison, T. F. Simplifying nickel(0) catalysis: an air-stable nickel precatalyst for the internally selective benzylation of terminal alkenes. *J. Am. Chem. Soc.* **135**, 1585–1592 (2013).
- Tang, J., Hackenberger, D. & Goossen, L. J. Branched arylalkenes from cinnamates: selectivity inversion in Heck reactions by carboxylates as decoupled directing groups. *Angew. Chem. Int. Ed.* **55**, 11296–11299 (2016).
- Tasker, S. Z., Gutierrez, A. C. & Jamison, T. F. Nickel-catalyzed Mizoroki–Heck reaction of aryl sulfonates and chlorides with electronically unbiased terminal olefins: high selectivity for branched products. *Angew. Chem. Int. Ed.* **53**, 1858–1861 (2014).
- Zheng, C. & Stahl, S. S. Regioselective aerobic oxidative Heck reactions with electronically unbiased alkenes: efficient access to  $\alpha$ -alkyl vinylarenes. *Chem. Commun.* **51**, 12771–12774 (2015).
- Zou, Y. et al. Selective arylation and vinylation at the  $\alpha$  position of vinylarenes. *Chem. Eur. J.* **19**, 3504–3511 (2013).
- Beletskaya, I. P. & Cheprakov, A. V. The Heck reaction as a sharpening stone of palladium catalysis. *Chem. Rev.* **100**, 3009–3066 (2000).
- Heck, R. F. Palladium-catalyzed reactions of organic halides with olefins. *Acc. Chem. Res.* **12**, 146–151 (1979).
- Wucher, P. et al. Breaking the regioselectivity rule for acrylate insertion in the Mizoroki–Heck reaction. *Proc. Natl Acad. Sci. USA* **108**, 8955–8959 (2011).
- Garnes-Portolés, F. et al. Regioirregular and catalytic Mizoroki–Heck reactions. *Nat. Catal.* **4**, 293–303 (2021).
- Bhakta, S. & Ghosh, T. Emerging nickel catalysis in Heck reactions: recent developments. *Adv. Synth. Catal.* **362**, 5257–5274 (2020).

29. Lin et al. Comparing nickel- and palladium-catalyzed Heck reactions. *Organometallics* **23**, 2114–2123 (2004).
30. Inamoto, K. et al. Synthesis and catalytic activity of a pincer-type bis(imidazolylidene) nickel(II) complex. *Organometallics* **25**, 3095–3098 (2006).
31. Ananikov, V. P. Nickel: the “spirited horse” of transition metal catalysis. *ACS Catal.* **5**, 1964–1971 (2015).
32. Badir, S. O. & Molander, G. A. Developments in photoredox/nickel dual-catalyzed 1,2-difunctionalizations. *Chem* **6**, 1327–1339 (2020).
33. Huang, H., Jia, K. & Chen, Y. Radical decarboxylative functionalizations enabled by dual photoredox catalysis. *ACS Catal.* **6**, 4983–4988 (2016).
34. Lang, X., Zhao, J. & Chen, X. Cooperative photoredox catalysis. *Chem. Soc. Rev.* **45**, 3026–3038 (2016).
35. Liu, J. et al. Visible-light-induced triple catalysis for a ring-opening cyanation of cyclopropyl ketones. *Chem. Commun.* **56**, 11508–11511 (2020).
36. Liu, Y.-Y., Liang, D., Lu, L.-Q. & Xiao, W.-J. Practical heterogeneous photoredox/nickel dual catalysis for C–N and C–O coupling reactions. *Chem. Commun.* **55**, 4853–4856 (2019).
37. Lu, F.-D., Lu, L.-Q., He, G.-F., Bai, J.-C. & Xiao, W.-J. Enantioselective radical carbocyanation of 1,3-dienes via photocatalytic generation of allylcopper complexes. *J. Am. Chem. Soc.* **143**, 4168–4173 (2021).
38. Mega, R. S., Duong, V. K., Noble, A. & Aggarwal, V. K. Decarboxylative conjugative cross-coupling of vinyl boronic esters using metallaphotoredox catalysis. *Angew. Chem. Int. Ed.* **59**, 4375–4379 (2020).
39. Peng, L., Li, Z. & Yin, G. Photochemical nickel-catalyzed reductive migratory cross-coupling of alkyl bromides with aryl bromides. *Org. Lett.* **20**, 1880–1883 (2018).
40. Prier, C. K., Rankic, D. A. & MacMillan, D. W. C. Visible light photoredox catalysis with transition metal complexes: applications in organic synthesis. *Chem. Rev.* **113**, 5322–5363 (2013).
41. Skubi, K. L., Blum, T. R. & Yoon, T. P. Dual catalysis strategies in photochemical synthesis. *Chem. Rev.* **116**, 10035–10074 (2016).
42. Tu, H.-Y., Zhu, S., Qing, F.-L. & Chu, L. Recent advances in nickel-catalyzed three-component difunctionalization of unactivated alkenes. *Synthesis* **52**, 1346–1356 (2020).
43. Twilton, J. et al. The merger of transition metal and photocatalysis. *Nat. Rev. Chem.* **1**, 0052 (2017).
44. Xi, X. et al. From esters to ketones via a photoredox-assisted reductive acyl cross-coupling strategy. *Angew. Chem. Int. Ed.* **61**, e202114731 (2022).
45. Yu, X.-Y., Zhao, Q.-Q., Chen, J., Chen, J.-R. & Xiao, W.-J. Copper-catalyzed radical cross-coupling of redox-active oxime esters, styrenes, and boronic acids. *Angew. Chem. Int. Ed.* **57**, 15505–15509 (2018).
46. Zhu, C., Yue, H., Chu, L. & Rueping, M. Recent advances in photoredox and nickel dual-catalyzed cascade reactions: pushing the boundaries of complexity. *Chem. Sci.* **11**, 4051–4064 (2020).
47. Zhu, C. et al. A multicomponent synthesis of stereodefined olefins via nickel catalysis and single electron/triplet energy transfer. *Nat. Catal.* **2**, 678–687 (2019).
48. Buzzetti, L., Prieto, A., Roy, S. R. & Melchiorre, P. Radical-based C–C bond-forming processes enabled by the photoexcitation of 4-alkyl-1,4-dihydropyridines. *Angew. Chem. Int. Ed.* **56**, 15039–15043 (2017).
49. Chen, Y., Wang, X., He, X., An, Q. & Zuo, Z. Photocatalytic dehydroxymethylative arylation by synergistic cerium and nickel catalysis. *J. Am. Chem. Soc.* **143**, 4896–4902 (2021).
50. Cong, F., Lv, X.-Y., Day, C. S. & Martin, R. Dual catalytic strategy for forging  $sp^2$ – $sp^3$  and  $sp^3$ – $sp^3$  architectures via  $\beta$ -scission of aliphatic alcohol derivatives. *J. Am. Chem. Soc.* **142**, 20594–20599 (2020).
51. Derosa, J., Apolinar, O., Kang, T., Tran, V. T. & Engle, K. M. Recent developments in nickel-catalyzed intermolecular dicarbofunctionalization of alkenes. *Chem. Sci.* **11**, 4287–4296 (2020).
52. Diallo, A. G. et al. Dual Ni/organophotoredox catalyzed allylative ring opening reaction of oxabenzonorbornadienes and analogs. *ACS Catal.* **12**, 3681–3688 (2022).
53. García-Domínguez, A., Mondal, R. & Nevado, C. Dual photoredox/nickel-catalyzed three-component carbonyl functionalization of alkenes. *Angew. Chem. Int. Ed.* **58**, 12286–12290 (2019).
54. Goddard, J.-P., Ollivier, C. & Fensterbank, L. Photoredox catalysis for the generation of carbon centered radicals. *Acc. Chem. Res.* **49**, 1924–1936 (2016).
55. Guan, H., Zhang, Q., Walsh, P. J. & Mao, J. Nickel/photoredox-catalyzed asymmetric reductive cross-coupling of racemic  $\alpha$ -chloro esters with aryl iodides. *Angew. Chem. Int. Ed.* **59**, 5172–5177 (2020).
56. Gui, Y.-Y., Sun, L., Lu, Z.-P. & Yu, D.-G. Photoredox sheds new light on nickel catalysis: from carbon–carbon to carbon–heteroatom bond formation. *Org. Chem. Front.* **3**, 522–526 (2016).
57. Kariofillis, S. K., Shields, B. J., Tekle-Smith, M. A., Zacuto, M. J. & Doyle, A. G. Nickel/photoredox-catalyzed methylation of (hetero)aryl chlorides using trimethyl orthoformate as a methyl radical source. *J. Am. Chem. Soc.* **142**, 7683–7689 (2020).
58. Lau, S. H. et al. Ni/photoredox-catalyzed enantioselective cross-electrophile coupling of styrene oxides with aryl iodides. *J. Am. Chem. Soc.* **143**, 15873–15881 (2021).
59. Marzo, L., Pagire, S. K., Reiser, O. & König, B. Visible-light photocatalysis: does it make a difference in organic synthesis? *Angew. Chem. Int. Ed.* **57**, 10034–10072 (2018).
60. Milligan, J. A., Phelan, J. P., Badir, S. O. & Molander, G. A. Alkyl carbon–carbon bond formation by nickel/photoredox cross-coupling. *Angew. Chem. Int. Ed.* **58**, 6152–6163 (2019).
61. Shu, W. et al. Ni-catalyzed reductive dicarbofunctionalization of nonactivated alkenes: scope and mechanistic insights. *J. Am. Chem. Soc.* **141**, 13812–13821 (2019).
62. Wei, X., Shu, W., García-Domínguez, A., Merino, E. & Nevado, C. Asymmetric Ni-catalyzed radical relayed reductive coupling. *J. Am. Chem. Soc.* **142**, 13515–13522 (2020).
63. Yang, T., Chen, X., Rao, W. & Koh, M. J. Broadly applicable directed catalytic reductive difunctionalization of alkenyl carbonyl compounds. *Chem* **6**, 738–751 (2020).
64. Zhu, S., Zhao, X., Li, H. & Chu, L. Catalytic three-component dicarbofunctionalization reactions involving radical capture by nickel. *Chem. Soc. Rev.* **50**, 10836–10856 (2021).
65. Liu, K. & Studer, A. Direct  $\alpha$ -acylation of alkenes via N-heterocyclic carbene, sulfinate, and photoredox cooperative triple catalysis. *J. Am. Chem. Soc.* **143**, 4903–4909 (2021).
66. Lu, Q. et al. Aerobic oxysulfonylation of alkenes leading to secondary and tertiary  $\beta$ -hydroxysulfones. *Angew. Chem. Int. Ed.* **52**, 7156–7159 (2013).
67. Meyer, A. U., Straková, K., Slanina, T. & König, B. Eosin Y (EY) photoredox-catalyzed sulfonylation of alkenes: scope and mechanism. *Chem. Eur. J.* **22**, 8694–8699 (2016).
68. Mulina, O. M., Ilovaisky, A. I., Parshin, V. D. & Terent'ev, A. O. Oxidative sulfonylation of multiple carbon-carbon bonds with sulfonyl hydrazides, sulfonic acids and their salts. *Adv. Synth. Catal.* **362**, 4579–4654 (2020).
69. Zhao, Q.-Q. et al. Photogenerated neutral nitrogen radical catalyzed bifunctionalization of alkenes. *Chem. Eur. J.* **25**, 8024–8029 (2019).
70. Mantry, L., Maayuri, R., Kumar, V. & Gandeepan, P. Photoredox catalysis in nickel-catalyzed C–H functionalization. *Beilstein J. Org. Chem.* **17**, 2209–2259 (2021).
71. Tellis, J. C., Primer, D. N. & Molander, G. A. Single-electron transmetalation in organoboron cross-coupling by photoredox/nickel dual catalysis. *Science* **345**, 433–436 (2014).
72. Yu, W., Chen, L., Tao, J., Wang, T. & Fu, J. Dual nickel- and photoredox-catalyzed reductive cross-coupling of aryl vinyl halides and unactivated tertiary alkyl bromides. *Chem. Commun.* **55**, 5918–5921 (2019).
73. Zultanski, S. L. & Fu, G. C. Nickel-catalyzed carbon–carbon bond-forming reactions of unactivated tertiary alkyl halides: Suzuki arylations. *J. Am. Chem. Soc.* **135**, 624–627 (2013).
74. Biswas, S. & Weix, D. J. Mechanism and selectivity in nickel-catalyzed cross-electrophile coupling of aryl halides with alkyl halides. *J. Am. Chem. Soc.* **135**, 16192–16197 (2013).
75. Cavalcanti, L. N. & Molander, G. A. Photoredox catalysis in nickel-catalyzed cross-coupling. *Top. Curr. Chem.* **374**, 39–59 (2016).
76. Wang, S. et al. Enantioselective access to chiral aliphatic amines and alcohols via Ni-catalyzed hydroalkylations. *Nat. Commun.* **12**, 2771 (2021).
77. Wei, Y., Ben-zvi, B. & Diao, T. Diastereoselective synthesis of aryl C-glycosides from glycosyl esters via C–O bond homolysis. *Angew. Chem. Int. Ed.* **60**, 9433–9438 (2021).
78. Torborg, C. & Beller, M. Recent applications of palladium-catalyzed coupling reactions in the pharmaceutical, agrochemical, and fine chemical industries. *Adv. Synth. Catal.* **351**, 3027–3043 (2009).
79. Zhu, S.-F., Yu, Y.-B., Li, S., Wang, L.-X. & Zhou, Q.-L. Enantioselective hydrogenation of  $\alpha$ -substituted acrylic acids catalyzed by iridium complexes with chiral spiro aminophosphine ligands. *Angew. Chem. Int. Ed.* **51**, 8872–8875 (2012).
80. Jefford, C. W., Kubota, T. & Zaslona, A. Intramolecular carbenoid reactions of pyrrole derivatives. A total synthesis of ( $\pm$ )-ipalbidine. *Helv. Chim. Acta* **69**, 2048–2061 (1986).
81. Lavecchia, M. J., Puig de la Bellacasa, R., Borrell, J. I. & Cavasotto, C. N. Investigating molecular dynamics-guided lead optimization of EGFR inhibitors. *Biorg. Med. Chem.* **24**, 768–778 (2016).
82. Zadrozna, I., Kurkowska, J. & Makuch, I. Enzymatic and microbial method of preparation of optically active ( $\pm$ )-3-methyl-4-phenyl-4,5-dihydroisoxazole-4-carboxylic acid. *Synth. Commun.* **27**, 4181–4191 (1997).
83. Füllöp, F. The chemistry of 2-aminocycloalkancarboxylic acids. *Chem. Rev.* **101**, 2181–2204 (2001).
84. Li, P. et al. Iodine-catalyzed diazo activation to access radical reactivity. *Nat. Commun.* **9**, 1972 (2018).
85. Du, X. et al. Cobalt-catalyzed highly enantioselective hydrogenation of  $\alpha,\beta$ -unsaturated carboxylic acids. *Nat. Commun.* **11**, 3239 (2020).

86. Huihui, K. M. M. et al. Decarboxylative cross-electrophile coupling of *N*-hydroxyphthalimide esters with aryl iodides. *J. Am. Chem. Soc.* **138**, 5016–5019 (2016).
87. Cao, Z.-C. & Shi, Z.-J. Deoxygenation of ethers to form carbon–carbon bonds via nickel catalysis. *J. Am. Chem. Soc.* **139**, 6546–6549 (2017).
88. Sun, X. et al. The mechanisms of boronate ester formation and fluorescent turn-on in *ortho*-aminomethylphenylboronic acids. *Nat. Chem.* **11**, 768–778 (2019).
89. Wang, K., Ding, Z., Zhou, Z. & Kong, W. Ni-catalyzed enantioselective reductive diarylation of activated alkenes by domino cyclization/cross-coupling. *J. Am. Chem. Soc.* **140**, 12364–12368 (2018).
90. Yan, X.-B. et al. Ni-catalyzed hydroalkylation of olefins with *N*-sulfonyl amines. *Nat. Commun.* **12**, 5881 (2021).
91. Zhao, X. et al. Divergent aminocarbonylations of alkynes enabled by photoredox/nickel dual catalysis. *Angew. Chem. Int. Ed.* **60**, 26511–26517 (2021).

### Acknowledgements

We thank the European Research Council (Advanced Grant Agreement 692640, to A.S.) and the Alexander von Humboldt Foundation (postdoctoral fellowship to K.L.) for supporting this work.

### Author contributions

K.L., D.L. and A.S. designed and analysed the experiments. K.L. ran all experiments. K.L., D.L. and A.S. wrote the manuscript. All authors contributed to discussions.

### Funding

Open access funding provided by Westfälische Wilhelms-Universität Münster.

### Competing interests

The authors declare no competing interests.

### Additional information

**Supplementary information** The online version contains supplementary material available at <https://doi.org/10.1038/s44160-022-00101-9>.

**Correspondence and requests for materials** should be addressed to Armido Studer.

**Peer review information** *Nature Synthesis* thanks the anonymous reviewers for their contribution to the peer review of this work. Primary Handling Editor: Thomas West, in collaboration with the *Nature Synthesis* team.

**Reprints and permissions information** is available at [www.nature.com/reprints](http://www.nature.com/reprints).

**Publisher's note** Springer Nature remains neutral with regard to jurisdictional claims in published maps and institutional affiliations.



**Open Access** This article is licensed under a Creative Commons Attribution 4.0 International License, which permits use, sharing, adaptation, distribution and reproduction in any medium or format, as long as you give appropriate credit to the original author(s) and the source, provide a link to the Creative Commons license, and indicate if changes were made. The images or other third party material in this article are included in the article's Creative Commons license, unless indicated otherwise in a credit line to the material. If material is not included in the article's Creative Commons license and your intended use is not permitted by statutory regulation or exceeds the permitted use, you will need to obtain permission directly from the copyright holder. To view a copy of this license, visit <http://creativecommons.org/licenses/by/4.0/>.

© The Author(s) 2022